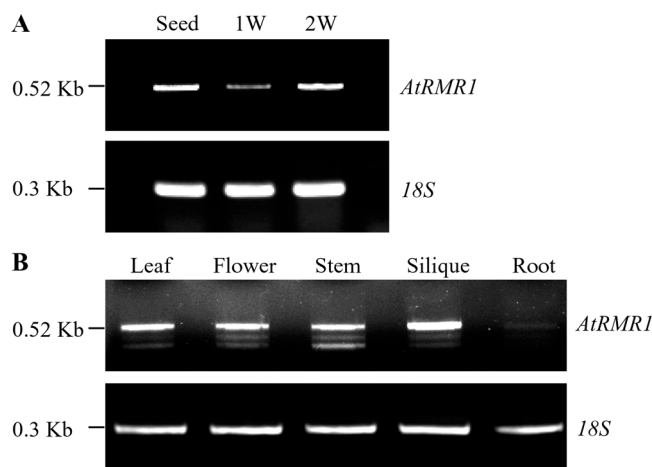


Park et al. <http://www.jcb.org/cgi/doi/10.1083/jcb.200504112>Spatial and temporal AtRMR1 expression patterns in *A. thaliana*

Sequence analysis revealed that the *A. thaliana* genome harbors six RMR homologues, named AtRMR1 to AtRMR6 (Fig. S1), that display 29–38% amino acid sequence homology to one another. RMR homologues that are encoded by JR700 and JR702, which are referred to here as AtRMR1 and AtRMR2,

AtRMR5	--MNYSWITIMSLLVICKLASA--KVVLIGKNTILSFDDVEATFTPIVRNSGECGILYVAE	57
AtRMR6	-----MFS-----APVVRSGEYGLLYAAE	20
AtRMR4	--MIRSSIVILSLLISHLYSA--KVLLIGNSTSLSFDDVEATFTPIKRSDQGGVLYVAE	57
AtRMR2	MM--RALVLLLYVCTVSCCLASS--KVILMRNMTLSFDDIEANFAPSVKGTGEIGVYVVAE	57
AtRMR3	MNLVLLILITLLLFIVSYVDAGQVILVDSNITRSFYDMEADFSPSVT--TVETGVVYVAE	59
AtRMR1	MRLVVSCLLVAAFLSLLRLVSLATVVLNLSIASFADLPKFDGSVTKNGICGALYVAD	60
	. . . . . * . . . . . * : * : *	
AtRMR5	PLEACSDITN--MAEKRSKYRSSYVLIVLGGCSFEKVRKAQKAGYKAAIVYNDGYDELL	115
AtRMR6	PLDACSYLTN--MAEKGSKFRPSYVLIVRGGCSFEKIRNAQEAGYKAAIVYNDRYEELL	78
AtRMR4	PLDACSDLVNTVNVKNGTTPSPYVLIIRGGCSFEDKIRNAQKAGYKAAIVYD--YED--	113
AtRMR2	PLDACQNLMM--KPEQSSNETSPFVLIIRGGCSFEKVRKAQKAGYKAAIYDNEGRGTL	115
AtRMR3	PLNACRLRN--KPEQSPVGTSPLVLIIRGGCSFEYKVRNAQRSGFKAAIVYDNDVDRNFL	117
AtRMR1	PLDGCSPLLHAAASNWTQHRTTKFALIIRGECSPEDKLLNAQNSGFQAVIYDNDNDL	120
	** : * : : : . . . . . ** : * * * * * : * : * : * : * : *	
AtRMR5	VPMAGNSSGVVDINGLLVTRASGEVLKGYADQDEMKLWLIP--GFGISSWSIMG--ITFISLL	173
AtRMR6	VRR--NSSGVYIHGVLVTRTSGEVLKEYTSRAEMELLIP--GFGISSWSIMA--ITFVSL	134
AtRMR4	-----FGFLVS--TTGEVLKEYAGRTDFEVWLMF--SFETSAWSIMA--ISFISLL	158
AtRMR2	IAMAGNSGGIRIHAVFTTKETGEVLKEYAGFPDTKVWLIP--SFENSAWSIMA--VSFISLL	173
AtRMR3	SAMGSDSDGIKIQAVFVTKRAGEMLKKYAGSEEMEVLVPPNTEDSVWSLYASIALILSL	177
AtRMR1	IYMKVNPQDITVDAVFVSNVAGEILLKYARGRDGECCLNP--PDRGSAWTVLA--ISFFSL	178
	. . . . . : * : * : * : * : * : * : * : * : *	
AtRMR5	AMSAILATCFVVRHRQIRQSVRDLPHGQGLSCMPRDLQSMPTVYSGVLEESSTSVTC	233
AtRMR6	VISAVLASVFSVRHRIRQHVRLDHHGGQGHSMRMPKDLLQSMPTVYTGVLGEGSTSVTC	194
AtRMR4	AMSAVLATCFVVRHRVRR--RRILALNGMDFHRMPKSMIIRMPPTIFNGICDEATTSLC	217
AtRMR2	AMSAVLATCFVVRHRIRR--RTSRSSRVREFHGMSSRLVKAMPSLIFSSFHEDNTTATC	232
AtRMR3	ALFCVMVTCVFFRYCSTI--RNSTS----QFNGMCRRTVKAMPSVTFTCAKIDNTTGFSC	232
AtRMR1	LIVTFLLIAPFAPRHWTTQWRGRHTR-----TIRLDKLVHTLPCFTFTDSAHKAG--ETC	232
	: : : : * : : : : : * : : : *	
AtRMR5	AICIDDDYCVGEKLRILPCKHKYHACIDSWLGRCSRFCPVCKQNPRTGNDVPPASETTPL	293
AtRMR6	AICIDDYRVGEILRILPCKHKYHACIDSWLGRCSRFCPVCKQNPRTGNDVPPASETTPL	254
AtRMR4	CICLENYKGDKLRILPCKHKFHVACVDLWLGRKSCFCPVCKRDARSISTDKPPSEHTPF	277
AtRMR2	AICLEDYTVGDKLRLLPCKHKFHAACVDSWLTSWRTFCPVCKRDARTSTGEPPASESTPL	292
AtRMR3	AICLEDYIVGDKLRVLPCKHKFHVACVDSWLTSWRTFCPVCKRDARTTADDEPLATESTPF	292
AtRMR1	AICLEDYRFGEISRLPQCQAHFLNCIDSWLTKWGTSCPVCKHDIRTETMSSEVHKRESP	292
	. ** : * : * : * : * : * : * : * : * : * : * : *	
AtRMR5	ISPSF-----NSITSLQS-----FYDLPIVVRVYL-----	318
AtRMR6	ISPGP-----NSITSLQS-----FYDLPIVVRVYL-----	279
AtRMR4	LSKTPSNTPTSSFLSSSTTPLQS-----SHELPISTRVDPSLPSTSMQPH	325
AtRMR2	LSSAASS-----FTSSSLHSSSVRSALLIGPSLGSLPTISFSPAYASSSYIRQS	342
AtRMR3	LSSSIAT-----SSLVCIDS-----PPLG---SSVSFSPAHSVSSFIHQF	329
AtRMR1	RTDTSTS-----RFAFAQSSQSR-----	310
	: : : : : : : : : : : : : : :	
AtRMR5	-----	
AtRMR6	-----	
AtRMR4	VPMYLSHSRSHTSFQNGSNRFSRPIVSRSSADLRNAVSRQSYNSPHQVSLPRLHRSYT	385
AtRMR2	FQSSSNRRSPPISVSRSSVDLRQQAASPSPPSQRSYISHIASPQSLGYPTISPFNTRYM	402
AtRMR3	VRSS-----PMNGSRISENLRRQAS--PLQSSSQRSLS--MKSSHSLGYSTMSPLNMG	381
AtRMR1	-----	
AtRMR5	-----	
AtRMR6	-----	
AtRMR4	HILGPGNASRSQVVGLLTSQREHSLHQNDSSRSFIHFASASSLPGW	431
AtRMR2	SPYRPSFNASFAMAGSSNYPLNPLRYSESAGTFSFYASANSPLDC	448
AtRMR3	SPYRPSFNASFGLFSSTNHLS-----NYTANTFSHFASANSPLD-	422
AtRMR1	-----	

Figure S1. **Sequence alignment of AtRMR homologues.** AtRMR homologues were aligned by using Clustal W1.62. Asterisks indicate conserved amino residues among the six RMR homologues. Numbers on the right indicate amino acid positions of the proteins. AtRMR1, At5g66160 (JR700); AtRMR2, At1g71980 (JR702); AtRMR3, At1g22670; AtRMR4, At1g09560; AtRMR5, At1g35630; AtRMR6, At1g35625.



**Figure S2. Tissue-specific and temporal expression patterns of *AtRMR1* in *A. thaliana*.** Total RNA was extracted from plants at different growth stages (A) or from different tissues (B) and subjected to semiquantitative RT-PCR for *AtRMR1*. PCR products from 18S rRNA served as an internal standard. The nucleotide sequence of the PCR products (0.52 kb) was confirmed by sequencing. 1W, 1 wk; 2W, 2 wk.

respectively, were previously shown to be expressed in root tip cells of *A. thaliana* (Jiang et al., 2000). To understand the biological role of these AtRMRs in intracellular trafficking, we decided to specifically study AtRMR1, which is a polypeptide of 32 kD. First, we examined its temporal and tissue-specific expression patterns by semiquantitative RT-PCR analysis using *AtRMR1*-specific primers. Total RNA was prepared from imbibed seeds, 1- and 2-wk-old *A. thaliana* plants, and from leaves, flowers, stems, siliques, and root tissues. The 18S ribosomal RNA level served as a control. The *AtRMR1* transcript was detected at similar levels at different growth stages (Fig. S2 A). In addition, *AtRMR1* was expressed at similar levels in all of the different tissues except for in the roots, in which it was expressed at significantly lower levels (Fig. S2 B). Thus, *AtRMR1* is expressed in most *A. thaliana* cells regardless of the growth stage of the plant.

#### Isolation of genomic DNA

1 g of leaf tissues that were harvested from 3-wk-old *A. thaliana* (Columbia) and tobacco (*Nicotiana tabacum*) plants were ground thoroughly in liquid N<sub>2</sub>. Lysis buffer (50 mM Tris, pH 7.5, 100 mM NaCl, 50 mM EDTA, 0.5% [wt/vol] SDS, and 10 mM β-mercaptoethanol) was then added. After 1 h, the sample was centrifuged, and the supernatant was extracted by phenol/chloroform. Genomic DNA was precipitated with ethanol.

#### RT-PCR analysis

Total RNA was extracted from imbibed seeds, cotyledons from 1-wk-old plants, and leaf tissues from 2-wk-old plants by using the TRIzol LS reagent (Invitrogen) according to the manufacturer's instructions. cDNA was synthesized from 1 μg of total RNA with Superscript II-RNase H reverse transcriptase (Invitrogen), and PCR was performed with the 5'-AT-GAGACTCGTCTGCTCA-3' and 5'-CGCGTACTTTCTCAAAAT-3' primers for the LU of *AtRMR1*. The 5'-ATGATAACTCGACGGATCGC-3' and 5'-CCTCCAATGGATCCTCGTTA-3' primers for 18S rRNA were used for 30 and 16 cycles, respectively, at 94, 48, and 72°C for 30 s.

#### Characterization of anti-RMR1 antibody

First, we examined the specificity of the anti-AtRMR1 antibody using protein extracts that were obtained from wild-type plants and protoplasts transformed with *AtRMR1-HA* (Fig. S3 A; Jin et al., 2001). The antibody specifically recognized a protein band of 32 kD in wild-type protein extracts and two bands of 32 and 33 kD from protein extracts that were obtained from *AtRMR1-HA*-transformed protoplasts (Fig. S3 B). The 33-kD band was also specifically detected with the anti-HA antibody. In contrast, the preimmune serum did not detect any protein. These results indicate that the anti-AtRMR1 antibody specifically recognizes AtRMR1. As a control, we used anti-AtRMR2 antibody raised against the COOH-terminal peptide of AtRMR2 (Jiang et al., 2000). The anti-AtRMR2 antibody specifically detected a 48-kD band corresponding to that of AtRMR2 (Fig. S3 C). To further test the specificity of anti-AtRMR1 antibody, we expressed AtRMR3 and AtRMR4 tagged with HA in protoplasts and examined their reactivity with this antibody. Although the anti-HA antibody specifically detected bands of 46 and 47 kD, which corresponded to AtRMR3 and AtRMR4, respectively, the anti-AtRMR1 antibody did not recognize these bands (Fig. S3 C), indicating that the anti-AtRMR1 antibody is specific for AtRMR1. Next, we examined whether AtRMR1 is modified by glycosyla-

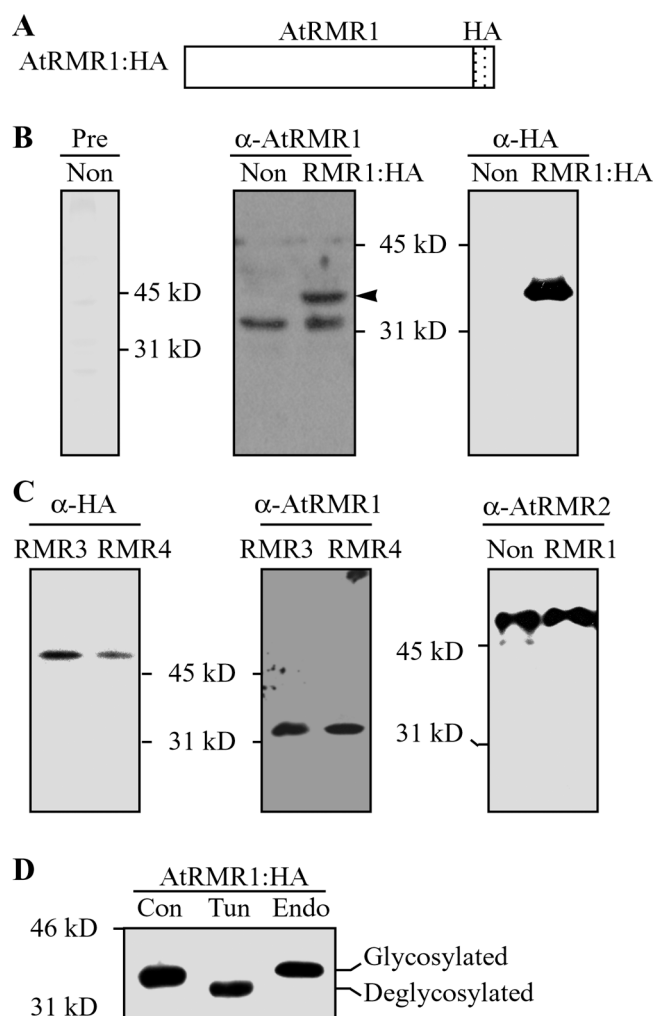


**Figure S3. Western blot analysis of endogenous and transiently expressed AtRMR1.** (A) Schematic depiction of the construct used. AtRMR1 was epitope-tagged with HA at their COOH terminus. (B) Western blot analysis. Protein extracts were obtained from untransformed (Non) and *AtRMR1-HA*-transformed (RMR1:HA) protoplasts and subjected to Western blot analysis using anti-AtRMR1 (α-AtRMR1) and anti-HA (α-HA) antibodies. As a control, preimmune serum (Pre) was used to stain the Western blot. Arrowhead indicates transiently expressed AtRMR1-HA. (C) Specificity of anti-AtRMR1 antibody. Protein extracts were prepared from untransformed protoplasts (Non) and protoplasts transformed with *AtRMR1-HA* (RMR1), *AtRMR3-HA* (RMR3), or *AtRMR4-HA* (RMR4) and were used for Western blot analysis using anti-AtRMR1 (α-AtRMR1) or anti-RMR2 (α-AtRMR2) antibodies. (D) AtRMR1-HA glycosylation pattern. Protoplasts were transformed with *AtRMR1-HA* and incubated in the presence (Tun) and absence (Con) of tunicamycin. Protein extracts that were obtained from untreated protoplasts were also digested with endoH (Endo). These protein extracts were subsequently analyzed by Western blot analysis using anti-HA antibody.

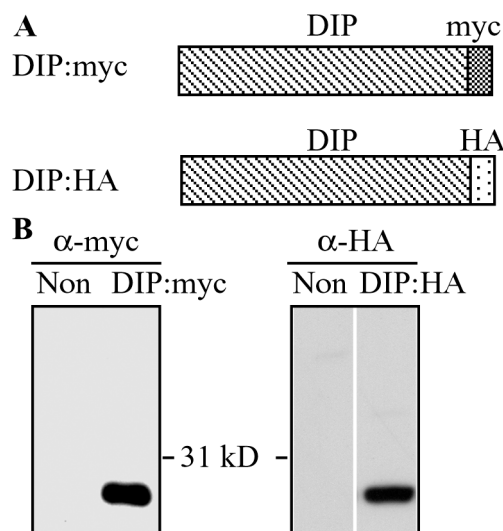


Figure S4. **Transient expression of epitope-tagged DIP in *A. thaliana* protoplasts.** (A) Schematic depiction of the constructs used. DIP was epitope-tagged with HA or myc at the COOH terminus. (B) Expression of myc- and HA-tagged DIP in protoplasts. Protein extracts were prepared from protoplasts that were transformed with *DIP-myc* or *DIP-HA* and were used for Western blot analysis using anti-myc ( $\alpha$ -myc) or anti-HA ( $\alpha$ -HA) antibodies, respectively. Non, untransformed protoplasts.

tion. Protein extracts were prepared from protoplasts expressing AtRMR1-HA in the presence and absence of tunicamycin, which is an inhibitor of  $\text{NH}_2$  glycosylation (Leavitt et al., 1977). AtRMR1-HA that was prepared from tunicamycin-treated protoplasts migrated faster than that prepared from untreated protoplasts (Fig. S3 D). Thus, AtRMR1-HA is glycosylated in *A. thaliana* leaf protoplasts. Then, we examined the endoH sensitivity of the  $\text{NH}_2$  glycan moiety on AtRMR1-HA (Kornfeld and Kornfeld 1985; Crofts et al., 1999). EndoH treatment did not change the mobility of AtRMR1-HA (Fig. S3 D), which suggests that the  $\text{NH}_2$  glycan moiety of AtRMR1-HA is the Golgi-modified complex type.

## References

- Crofts, A.J., N. Leborgne-Castel, S. Hillmer, D.G. Robinson, B. Phillipson, L.E. Carlsson, D.A. Ashford, and J. Denecke. 1999. Saturation of the endoplasmic reticulum retention machinery reveals anterograde bulk flow. *Plant Cell*. 11:2233–2248.
- Jiang, L., T.E. Phillips, S.W. Rogers, and J.C. Rogers. 2000. Biogenesis of the protein storage vacuole crystalloid. *J. Cell Biol.* 150:755–770.
- Jin, J.B., Y.A. Kim, S.J. Kim, S.H. Lee, D.H. Kim, G.W. Cheong, and I. Hwang. 2001. A new dynamin-like protein, ADL6, is involved in trafficking from the trans-Golgi network to the central vacuole in *Arabidopsis*. *Plant Cell*. 13:1511–1526.
- Kornfeld, R., and S. Kornfeld. 1985. Assembly of asparagine-linked oligosaccharides. *Annu. Rev. Biochem.* 54:631–664.
- Leavitt, R., S. Schlesinger, and S. Kornfeld. 1977. Tunicamycin inhibits glycosylation and multiplication of Sindbis and vesicular stomatitis viruses. *J. Virol.* 21:375–385.

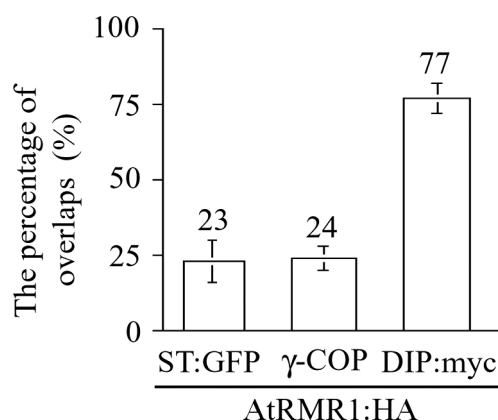


Figure S5. **Quantification of the overlap of AtRMR1-HA with ST-GFP,  $\gamma$ -COP, or DIP-myc.** The number of AtRMR1-positive punctate stains that colocalized with ST-GFP,  $\gamma$ -COP, or DIP-myc-positive punctate stains were counted to estimate the degree of overlap. More than 200 punctate stains were counted for each comparison. Three independent experiments were performed to obtain means and SEM (error bars).

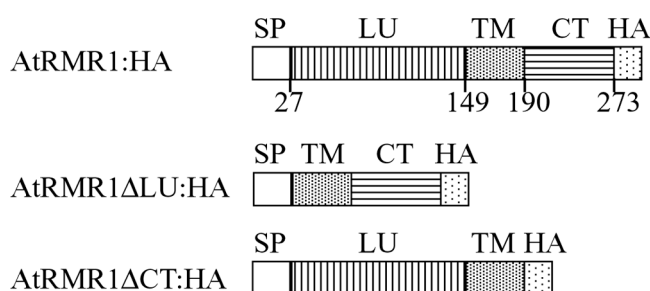


Figure S6. **Schematic depiction of the constructs used.** The LU and COOH-terminal ring H2 domains of AtRMR1 were deleted in AtRMR1ΔLU-HA and AtRMR1ΔCT-HA, respectively. Numbers indicate amino acid positions of AtRMR1. SP, leader sequence; LU, luminal domain; TM, transmembrane domain; CT, ring H2 finger domain.